


Phase noise to amplitude noise conversion between statistically independent optical fieldsArielle Little, Michael Huang, and James Camparo ^{*}*Physical Sciences Laboratories, The Aerospace Corporation, 2310 East El Segundo Boulevard, El Segundo, California 90245, USA*

(Received 23 November 2022; accepted 16 February 2023; published 17 March 2023)

Pump-probe experiments are ubiquitous in atomic, molecular, and optical physics, where a strong pump field induces some change in a quantum system that is probed by a much weaker field. Often, high intensity of the pump field is at a premium with all other characteristics of the strong field subordinate. As a particular example, of relevance to atomic clocks and atomic magnetometers, a strong broad-linewidth laser optically pumps an atomic vapor, which is then probed by a much weaker narrow-linewidth laser. Though the broad-linewidth field suffers laser phase noise (PM) to amplitude noise (AM) conversion, the narrow-linewidth probe *by itself* produces a much quieter signal. Here, we consider the question of whether the noisy pump field maps its (PM-to-AM) absorption cross-section fluctuations onto the quiet probe field's transmission. Our results show that PM-to-AM noise does *not* transfer directly: atoms interacting with the pump field are instantaneously distinct from those interacting with the probe field. However, the broad-linewidth laser can influence the quiet field's transmission through the vapor due to optical pumping, resulting in fluctuations in the number density of atoms in the absorbing states. Nevertheless, there is a saving grace for this "PM-to-AM induced optical pumping" noise transfer: for very high noisy-field intensities (where optical pumping saturates) this type of noise on the probe field becomes negligible.

DOI: [10.1103/PhysRevA.107.033109](https://doi.org/10.1103/PhysRevA.107.033109)**I. INTRODUCTION**

Though the absorption cross section of an atom is often thought to be an intrinsic constant of atomic structure, it actually derives from *dynamical* features of the field-atom interaction [1]. Only when the field is monochromatic and of constant amplitude does the absorption cross section become time *independent*, taking on the appearance of a parameter solely determined by atomic structure [2]. A particularly illuminating illustration of this occurs for dipole transitions induced by short-pulse lasers, where experiments have shown that an atomic vapor's ability to absorb electromagnetic radiation only "turns on" after the induced dipole moments of the atoms evolve into steady state [3]; at shorter times the vapor is effectively transparent. Stated more carefully, an atomic vapor's absorption cross section is a collective manifestation of (field-created) atomic dipole moments [4,5], and these dipole moments only come into existence when the bare-atom eigenstates of the atom [6] evolve into an atomic superposition state.

Of increasing interest over the past decade has been the dynamical response of quantum systems to *randomly* fluctuating fields, since (on the one hand) no field in nature is truly monochromatic, and (on the other) the stochastic field-atom interaction can have much richer physics than that appearing in standard textbooks [7,8]. As examples, Papoyan and Shmavonyan have found that when a resonant dipole transition is excited by a cw phase-diffusion field the Fourier spectrum of the transmitted laser intensity contains components

near the transition's Rabi frequency [9]. The field-atom interaction becomes even richer when three-level systems are considered [10,11], and for the case of nonlinear processes higher-order correlation functions for the field play increasingly significant roles in the quantum system's response to the field [12,13].

This dynamic character of the field-atom interaction is also behind laser phase noise (PM) to transmitted intensity noise (AM) conversion [14], which is now known to be an important noise process in quantum devices employing diode lasers for signal generation [15,16]. Briefly, an individual atom's induced dipole moment has a dependence on the phase of the electromagnetic field [17]. Consequently, as the field's phase varies so too does the atom's dipole moment. Since the media of typical laboratory experiments have wavefront propagation times much shorter than the timescale of a typical laser's phase fluctuations [18], all atoms in the vapor experience the same laser phase. Thus, as the individual atoms' induced dipole moments fluctuate with the laser phase there appear random variations in the vapor's absorption cross section; as the vapor's absorption cross section fluctuates, so too does the transmitted laser intensity: in a phrase, laser PM-to-AM noise conversion. Importantly, PM-to-AM noise conversion is fundamental to the field-atom interaction; it is unavoidable. PM-to-AM must take place at some level whenever resonant light passes through an absorbing medium. Consequently, in quantum devices it can only be partially mitigated through various experimental manipulations, routinely through the use of very narrow-linewidth lasers [19] but also with the addition of rapid collision broadening [17].

Though much has been discovered regarding PM-to-AM conversion and its influence on quantum devices, there is a

^{*}james.c.camparo@aero.org

fundamental atomic physics question that has yet to be addressed: Can PM-to-AM noise induced by one optical field be transferred to another independent optical field? To be more specific, does PM-to-AM noise conversion arising from a “phase-noisy” field map onto the transmitted light of a field having (by itself) little to no PM-to-AM noise conversion? On the one hand, viewing PM-to-AM conversion in terms of a vapor’s absorption cross-section fluctuations, one would answer this question in the affirmative: as the phase-noisy field creates absorption cross-section fluctuations throughout the vapor, those variations will be sensed by any resonant field propagating through the vapor no matter how “phase quiet” the field may be on its own. However, viewing PM-to-AM noise conversion in terms of the individual atoms’ induced dipole moments, one would answer this question in the negative: those atoms interacting with the phase-noisy field are different from those interacting with the phase-quiet field, and so there is no PM-to-AM transfer between independent fields. While this question has important implications for a number of quantum devices, the issue of PM-to-AM noise conversion translates to all manner of pump-probe experiments in atomic, molecular, and optical (AMO) physics: single-photon probing of atomic structure [20], excited-state absorption of rare-earth ions [21], and the study of velocity-preserving excited-state transfer in vapors [22], to name just a few.

In the following sections we experimentally address this question using a vertical-cavity surface emitting laser (VCSEL) as our phase-noisy field and light from an rf-discharge lamp as our phase-quiet field. Though the resonant light from an alkali rf-discharge lamp will have a linewidth of several gigahertz [23,24], while VCSELs have linewidths of ~ 50 – 100 MHz [25,26], the phase fluctuations of the lamp are in a sense so fast that the atoms are unable to follow them. Consequently, alkali rf-discharge lamps do not exhibit PM-to-AM noise conversion to any significant extent [27] and can be considered a phase-quiet field since the atomic system only perceives the lamp field’s average temporal phase.

In the next section we describe our experimental arrangement examining this question, and following that are our results looking for PM-to-AM noise conversion in the transmitted resonant lamplight. Regarding the question that motivated these studies, we will show that PM-to-AM noise *does not* transfer directly between independent optical fields. Thus, the phase-noisy field does not create absorption cross section fluctuations throughout the vapor, but only for that subset of atoms instantaneously interacting with the phase-noisy field. However, we will find that there is another manifestation of PM-to-AM noise that *does* transfer: PM-to-AM induced optical pumping noise. As the phase-noisy VCSEL optically pumps the alkali vapor, it produces fluctuations in the number density of atoms in the vapor’s optically absorbing states. Though the phase-quiet field’s absorption cross section does not fluctuate as a consequence of direct PM-to-AM transfer, the number density of atoms in the absorbing state does fluctuate, and this manifests as noise in the phase-quiet field’s transmission through the vapor. In the final section, we discuss a simple model of PM-to-AM induced optical pumping noise that validates our interpretation of the experimental results.

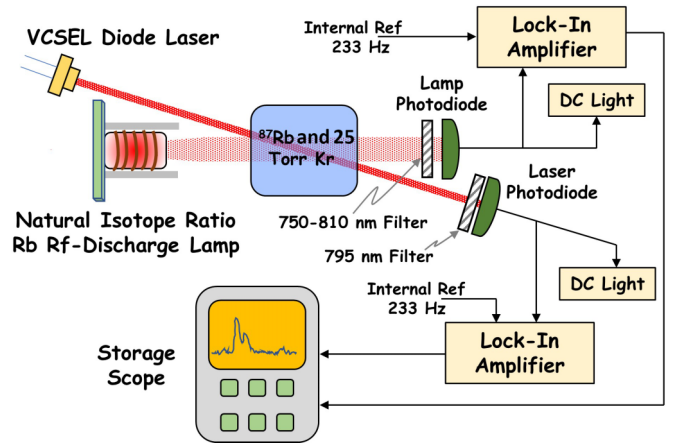


FIG. 1. Block diagram of our experimental arrangement. The light beam from a VCSEL diode laser overlaps the light from a natural isotope Rb rf-discharge lamp in an absorption cell containing isotopically enriched ^{87}Rb along with 25 Torr of Kr. Not shown is a linear polarizer that allows attenuation of the diode laser light reaching the resonance cell.

II. EXPERIMENT

Figure 1 is a block diagram of our experimental arrangement. An isotopically enriched vapor of ^{87}Rb is contained in a glass cell of length $L = 4.2$ cm and diameter $D = 2.5$ cm along with 25 Torr of Kr as a buffer gas. A VCSEL diode laser excites the D_1 resonance of Rb at 795 nm: $5^2S_{1/2} \rightarrow 5^2P_{1/2}$. The laser beam passing through the cell has a diameter of approximately 0.7 cm (0.4 cm at cell entrance and 0.9 cm at cell exit), and the lamplight has a diameter throughout the resonance cell of about 1.7 cm. Lamplight is derived from a natural isotope-ratio rf-discharge lamp.

The cell is nominally maintained at a temperature of 37°C , so that the Rb number density ($[\text{Rb}]$) in the vapor is approximately $4 \times 10^{10} \text{ cm}^{-3}$, and we measured the vapor’s attenuation coefficient for *laser light* as $[\text{Rb}]\sigma L = 0.34$ for excitation out of $|^{87}\text{Rb}(F_g = 2)\rangle$ and 0.19 for excitation out of $|^{87}\text{Rb}(F_g = 1)\rangle$. Here, $I(L) = I_0 e^{-[\text{Rb}]\sigma L}$, where $I(L)$ is the transmitted laser intensity and σ is the average absorption cross section. From knowledge of the Rb number density and $[\text{Rb}]\sigma L$ we estimate the absorption cross sections as $\sigma(F_g = 2) = 2.0 \times 10^{-12} \text{ cm}^2$ and $\sigma(F_g = 1) = 1.1 \times 10^{-12} \text{ cm}^2$. As these attenuation coefficients indicate, the vapor is optically thin for laser light in our experiments (i.e., $[\text{Rb}]\sigma L < 1$), and consequently (given the lamp’s broader spectral linewidth) also optically thin for the lamp. Though an optically thick vapor would likely have increased PM-to-AM conversion, having a thin vapor for both lamp and laser light decreases the potential for unanticipated systematic effects that might arise from different levels of nonlinear attenuation for the two fields.

The laser light is detected with a Si photodiode, whose signal is input to a lock-in amplifier internally referenced to a low modulation frequency (i.e., 233 Hz). As there is no modulated signal actually at this frequency, the lock-in essentially measures the noise at 233 Hz in a 1 Hz bandwidth, δV . This Fourier frequency for the noise was chosen since it

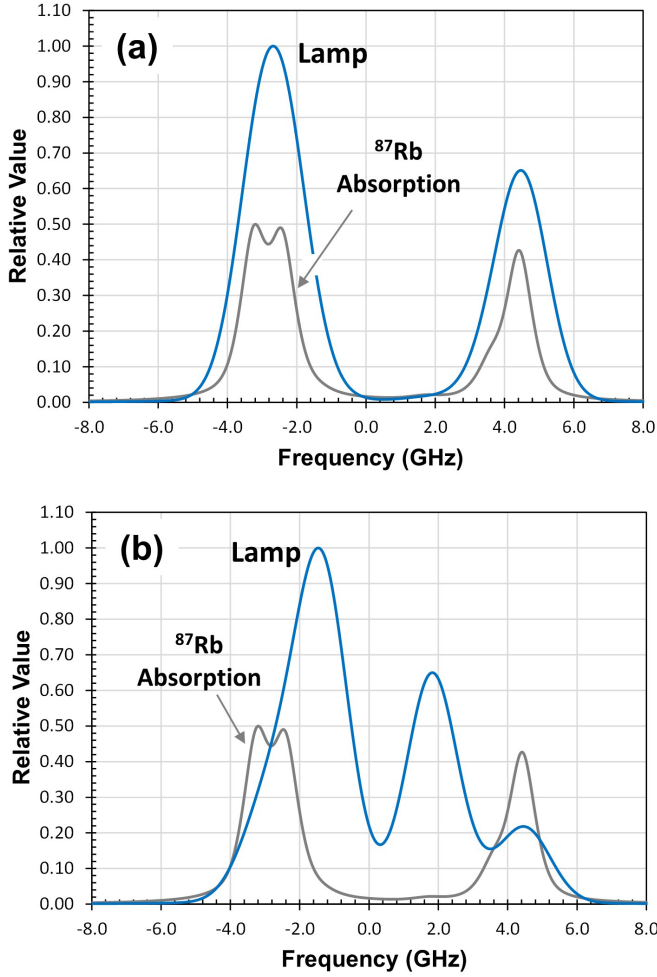


FIG. 2. (a) Computed spectrum for a pure ^{87}Rb lamp. (b) Computed spectrum for a natural isotope-ratio Rb lamp: we consider the leftmost lamp peak as $|e\rangle \rightarrow |^{87}\text{Rb}(F_g = 2)\rangle$, the middle lamp peak as $|e\rangle \rightarrow |^{85}\text{Rb}(F_g = 2)\rangle$, and the rightmost lamp peak as $|e\rangle \rightarrow |^{87}\text{Rb}(F_g = 1)\rangle$. For these calculated spectra we assumed a 1.6 GHz wide lamp line [24]. For the natural Rb lamp, most of the spectral intensity overlaps the lower-frequency ^{87}Rb absorption line [i.e., $5^2S_{1/2}(F_g = 2) \rightarrow |e\rangle$], with hardly any excitation of the higher-frequency $5^2S_{1/2}(F_g = 1) \rightarrow |e\rangle$ transition. Here, $|e\rangle$ corresponds to both the $5^2P_{1/2}$ and $5^2P_{3/2}$ states: 795 and 780 nm light, respectively.

corresponds to the general range of microwave modulation frequencies in many vapor-cell atomic clocks [28,29]. We also measure the average dc light reaching the photodiode: $\langle V \rangle$. Not shown in the figure is a linear polarizer that we rotate to vary the laser intensity entering the resonance cell. Relative intensity noise (RIN) is defined as $\delta V / \langle V \rangle$.

As mentioned above, our phase-quiet field is a natural isotope-ratio Rb rf-discharge lamp: 28% ^{87}Rb and 72% ^{85}Rb . An illustration of the lamp's computed spectrum is shown in Fig. 2, and as can be seen most of the lamplight comes from ^{85}Rb fluorescence. Using a spectrometer, we confirmed that the only light passing through our photodetector's bandpass filter was Rb 795 and 780 nm light: 60% 780 nm light and 40% 795 nm light. As the figure also shows, ^{85}Rb fluorescence preferentially excites atoms out of the ^{87}Rb $F_g = 2$ ground-state hyperfine level [30,31]. Thus, for the purposes

of anticipating the noise characteristics of the lamplight, we can approximate the lamp as emitting just four spectral lines; listed in order of increasing optical frequency we define the various transitions' rates of photon emission as

$$\left. \begin{aligned} 795 \text{ nm } r_A &\Rightarrow |e\rangle \rightarrow |^{87}\text{Rb}(F_g = 2)\rangle \\ 795 \text{ nm } r_B &\Rightarrow |e\rangle \rightarrow |^{85}\text{Rb}(F_g = 2)\rangle \\ 795 \text{ nm } r_C &\Rightarrow |e\rangle \rightarrow |^{87}\text{Rb}(F_g = 1)\rangle \end{aligned} \right\} 40\% \quad (1a)$$

$$780 \text{ nm } r_0 \Rightarrow |e\rangle \rightarrow |g\rangle \quad 60\%, \quad (1b)$$

with $r_A > r_B > r_C$. (Due to a coincidence of nature, r_A contains light emitted by both ^{85}Rb and ^{87}Rb ; however, we consider this in total as affecting the $|^{87}\text{Rb}(F_g = 2)\rangle$ level.) The lamplight is detected with its own photodetector, which is input to a lock-in amplifier also internally referenced to 233 Hz allowing measurement of the lamplight noise. We anticipate no laser-induced noise on the 780 nm D_2 lamplight reaching the photodetector since the laser is tuned to the 795 nm D_1 resonance only.

In order to anticipate the lamplight's RIN under the assumption that laser-induced PM-to-AM conversion *directly* affects the lamplight, we employ the Beer-Lambert law of exponential attenuation [32] to write the signal at the lamp's photodetector as

$$S_{\text{lamp}} = r_0 + r_A e^{-\rho_2 [\text{Rb}] (\sigma_{\text{dl}} + \delta\sigma_2) L} + r_B + r_C e^{-\rho_1 [\text{Rb}] (\sigma_{\text{dl}} + \delta\sigma_1) L}, \quad (2)$$

where ρ_j is the fractional population in the ^{87}Rb $|F_g = j\rangle$ state, σ_{dl} is the discharge lamp's (dl) absorption cross section [33], and the $\delta\sigma_1$ ($\delta\sigma_2$) correspond to the cross-section fluctuations arising from *laser* PM-to-AM conversion when the laser is tuned to excite atoms out of the $|F_g = 1\rangle$ state ($|F_g = 2\rangle$ state). Note that we have not assumed any attenuation of the 780 nm lamplight; this is likely a fair assumption given the optically thin nature of our vapor, but it also implies that our estimate of lamplight RIN will be something of a lower bound. Further, with the optically thin nature of the vapor we have $[\text{Rb}] \delta\sigma_j L \ll 1$. Thus, since the (possible) absorption cross-section fluctuations will only be associated with the 795 nm light (as this is the laser wavelength), we write the fluctuations in the lamplight signal as

$$\delta S_{\text{lamp}} = [\text{Rb}] L \{ r_A \rho_2 \delta\sigma_2 + r_C \rho_1 \delta\sigma_1 \}, \quad (3)$$

which gives rise to a lamplight RIN of

$$\begin{aligned} \text{RIN}_{\text{lamp}} &= \frac{[\text{Rb}] L \{ r_A \rho_2 \delta\sigma_2 + r_C \rho_1 \delta\sigma_1 \}}{r_0 + r_A + r_B + r_C} \\ &= \frac{2}{5} \frac{[\text{Rb}] L \{ r_A \rho_2 \delta\sigma_2 + r_C \rho_1 \delta\sigma_1 \}}{r_A + r_B + r_C}. \end{aligned} \quad (4)$$

In the absence of any optical pumping $\rho_2 = 5/8$ and $\rho_1 = 3/8$, so that Eq. (4) becomes

$$\text{RIN}_{\text{lamp}} = \frac{1}{4} [\text{Rb}] \sigma_L L \left\{ \frac{r_A \left(\frac{\delta\sigma_2}{\sigma_L} \right) + \frac{3}{5} r_C \left(\frac{\delta\sigma_1}{\sigma_L} \right)}{r_A + r_B + r_C} \right\}, \quad (5)$$

where σ_L is the absorption cross section for laser light. Similar considerations hold for the laser RIN, allowing us to

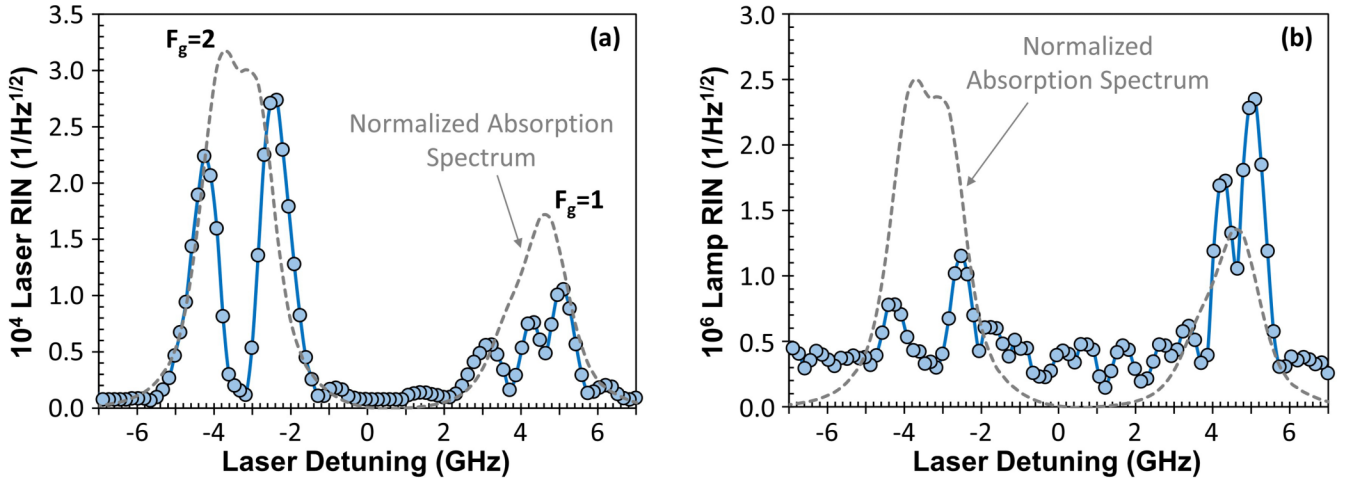


FIG. 3. (a) Laser RIN/Hz^{1/2} as a function of laser detuning showing the classical “M shape” of PM-to-AM conversion; (b) lamp RIN/Hz^{1/2} as a function of the laser’s detuning from resonance.

immediately write

$$\text{RIN}_{\text{laser}} = \frac{5}{8} [\text{Rb}] \sigma_L L \left\{ \left(\frac{\delta \sigma_2}{\sigma_L} \right) + \frac{3}{5} \left(\frac{\delta \sigma_1}{\sigma_L} \right) \right\}. \quad (6)$$

It is worth noting that given $\delta \sigma_1 \cong \delta \sigma_2$ and the fact that $r_A/r_C \sim 5$ [from the lamplight intensities shown in Fig. 2(b)], we expect the RIN *for lamplight* to be greater when the laser is tuned to the $|F_g = 2\rangle$ transition than when it is tuned to the $|F_g = 1\rangle$ transition by roughly a factor of $(5r_A/3r_C) \sim 8$. Alternatively, the RIN *for the laser* should only be larger by roughly a factor of 1.7 when the laser is tuned to $|F_g = 2\rangle$ compared to when it is tuned to $|F_g = 1\rangle$. Further, looking at the ratio of lamplight RIN to laser RIN we have (just considering the laser tuned to $F_g = 2$ for simplicity)

$$\frac{\text{RIN}_{\text{lamp}}}{\text{RIN}_{\text{laser}}} = \frac{2}{5} \left(\frac{r_A}{r_A + r_B + r_C} \right) \cong \frac{1}{5}, \quad (7)$$

where the final factor on the right comes from estimating the term in brackets after regarding Fig. 2(b).

Thus, there are three semiquantitative predictions that we can make *if* laser-induced PM-to-AM conversion transfers *directly* to lamplight transmission as a consequence of the two fields experiencing the same cross-section fluctuations:

(1) Regarding Eq. (5), lamplight RIN should be insensitive to the *laser’s* power level.

(2) Lamplight RIN should be larger with the laser tuned to the $|F_g = 2\rangle$ transition than to the $|F_g = 1\rangle$ transition by almost an order of magnitude.

(3) Lamplight RIN should be smaller than laser RIN by roughly 20%.

To the extent that these three predictions are borne out by experiment, we will have reasonable confidence that laser RIN transfers directly to the lamplight’s transmission. To the extent that none of these three predictions are borne out by experiment we must conclude that laser RIN does not transfer directly to the lamplight’s transmission.

III. RESULTS

Figure 3(a) shows the laser’s measured RIN as a function of laser detuning for one laser power (i.e., 305 μW). The laser’s RIN shows the classical “M shape” that is associated with PM-to-AM conversion [17], and as one would anticipate the peaks of the laser RIN occur near the inflection points of the absorption profile. Further, the RIN for the laser tuned to the $F_g = 1$ resonance is somewhat smaller than the RIN for the laser tuned to the $F_g = 2$ resonance, which is consistent with the previous discussion.

Figure 3(b) shows the lamp’s measured RIN as a function of the laser’s detuning. We first note that the lamp’s RIN for the laser tuned to $F_g = 1$ is greater than for the laser tuned to $F_g = 2$. This is opposite to our prediction if lamplight RIN were to result from a direct transfer of cross-section fluctuations to the lamplight’s transmission. Additionally, rather than lamplight RIN being about 20% smaller than the laser’s RIN, the RIN shown in Fig. 3(b) is two orders of magnitude smaller than the laser RIN. This is further illustrated in Fig. 4, where the peak RINs for the laser and lamp (examined over the full absorption spectrum) are shown as a function of laser power.

Figure 4 also indicates that the laser RIN and the lamplight RIN depend on the laser power. Specifically, the laser RIN appears to fall nearly linearly with laser power, while the lamplight RIN has a nonlinear dependence on laser power. This latter is again contrary to our predictions outlined in the previous section and is illustrated more clearly in Figs. 5(a) and 5(b). Together, these results provide convincing evidence that there is no *direct* transfer of laser PM-to-AM noise to lamplight transmission due to cross-section fluctuations. We must therefore conclude that the vapor-phase atoms involved in the attenuation of the laser field are separate and distinct from the atoms that are involved in the attenuation of the lamplight (at least in this low laser intensity regime). Nevertheless, we do observe a correlation between lamplight RIN and the laser’s resonant interaction with the vapor. If this cannot be attributed to absorption cross-section fluctuations directly, then it must be that the laser field’s cross-section fluctuations have an *indirect* influence on the lamplight’s

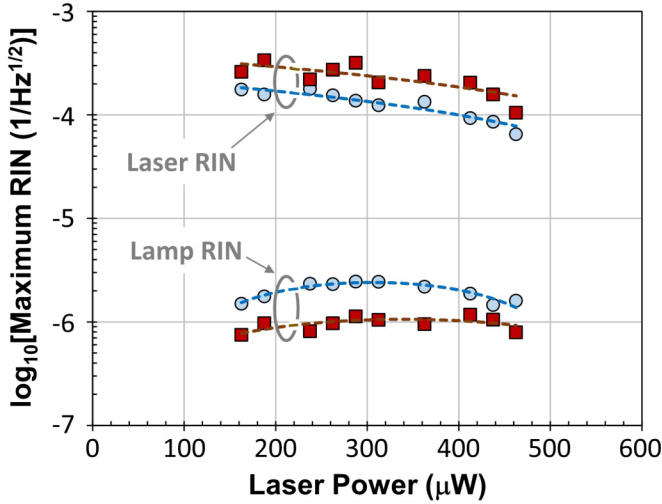


FIG. 4. Maximum RIN over the absorption spectrum for the laser and the lamp. In each case, circles correspond to the laser tuned to the $F_g = 1$ resonance, while squares correspond to the laser tuned to the $F_g = 2$ resonance.

transmission. As we argue subsequently, this indirect influence is due to PM-to-AM induced optical pumping noise.

IV. PM-TO-AM INDUCED OPTICAL PUMPING NOISE

Kitching *et al.* [34] were probably the first to recognize that PM-to-AM cross-section fluctuations could induce optical pumping noise. Though their focus was on the propagation of a bimodal field through an atomic vapor in a coherent-population-trapping (CPT) experiment, they nonetheless convincingly showed that field fluctuations resulted in optical pumping rate fluctuations. In turn, these yielded stochastic variations in the number of atoms in an absorbing state, and hence PM-to-AM *induced* optical pumping noise that affected the transmission of light through the resonant vapor.

To better establish that the laser-correlated lamplight noise observed in our experiments is also due to PM-to-AM induced optical pumping noise, and does not arise from direct PM-to-AM noise conversion, we first note that Fig. 5(a) shows a linear decrease in laser RIN with laser power. The RIN of standard PM to AM should be independent of laser power, since the cross-section fluctuations are independent of laser intensity [see Eq. (A13)]. Further evidence for optical pumping's role comes from Fig. 6, which shows lamplight RIN for the laser tuned to $|F_g = 1\rangle$ as a function of laser power, but now for a lower temperature of 30 °C. Consistent with previous research [14], as the vapor temperature is lowered the falloff in RIN due to optical pumping occurs at lower laser intensities.

A theory describing PM-to-AM induced optical pumping noise for two statistically independent fields is laid out in the Appendix, and to proceed we again write the lamplight signal at the photodetector in terms of the Beer-Lambert law of exponential attenuation [32]. Now, however, it is the fraction of atoms in the absorbing state ρ_2 that fluctuates (i.e., for the simple model described in the Appendix we assume that the

lamp only excites atoms out of $|F_g = 2\rangle$). Thus,

$$S_{\text{lamp}} = r_A e^{-\langle\rho_2\rangle + \delta\rho} [\text{Rb}] \sigma_{\text{dl}} L = r_A e^{-\langle\rho_2\rangle} [\text{Rb}] \sigma_{\text{dl}} L (1 - \delta\rho [\text{Rb}] \sigma_{\text{dl}} L). \quad (8)$$

Consequently, the RIN of the lamplight becomes

$$\text{RIN}_{\text{lamp}} = \sqrt{\langle\delta\rho^2\rangle} [\text{Rb}] \sigma_{\text{dl}} L, \quad (9)$$

where $\langle\delta\rho^2\rangle$ is given by Eq. (A12) in the Appendix along with Eqs. (A13) and (A14). We note that in the equation for $\langle\delta\rho^2\rangle$ the average fractional population in $|F_g = 2\rangle$ appears, $\langle\rho_2\rangle$. This is computed with the aid of Eq. (A8),

$$\langle\rho_2\rangle = \frac{\langle R_3 \rangle + \langle R_4 \rangle + 2\gamma}{\sum_{k=1}^4 \langle R_k \rangle + r_A + 4\gamma}, \quad (10)$$

where γ is the collisional hyperfine relaxation rate and the $\langle R_k \rangle$ are expressed as laser photon absorption rates for transitions k averaged over the cell length (i.e., R_3 and R_4 imply excitation out of $|F_g = 1\rangle$ to the two excited-state hyperfine levels, while R_1 and R_2 imply excitation out of $|F_g = 2\rangle$):

$$\langle R_k \rangle = \left(\frac{R_o \eta_k \Gamma^2}{\Gamma^2 + \Delta_k^2} \right) \frac{1 - e^{-[\text{Rb}] \sigma_k L}}{[\text{Rb}] \sigma_k L}. \quad (11)$$

In this expression, R_o is associated with the laser photon flux at the entrance to the resonance cell, η_k is the relative strength of the k th transition, Γ is the linewidth [half width at half maximum (HWHM)] of the optical transition, Δ_k is the detuning of the laser from the k th optical resonance, and $[\text{Rb}] \sigma_k L$ is the laser's attenuation coefficient for the k th transition at a particular resonance cell temperature.

To express the theoretical results in terms of laser power for comparison to experiment, we note that for a laser power of 100 μW at 795 nm our photon flux Φ is $1 \times 10^{15} \text{ cm}^{-2} \text{ s}^{-1}$. Given our estimated absorption cross section for the $F_g = 1$ resonance this implies a photon absorption rate of $\langle R_4 \rangle = 1100 \text{ s}^{-1}$. If we now assume that the hyperfine relaxation rate in our experiment is similar to that in our other experiments employing similar geometry cells and experimental conditions (i.e., $\gamma \sim 360 \text{ s}^{-1}$) [35] and taking $\eta_4 = 1.67$, we can calibrate R_o/γ : $R_o/\gamma = 1 \Rightarrow P_{\text{laser}} = 55 \mu\text{W}$.

Figure 7 shows RIN_{lamp} for $P_{\text{laser}} = 200 \mu\text{W}$ and a cell temperature of 37 °C. (Given the linewidths of the absorptions shown in Fig. 3 and the anticipated linewidth of our lamp's emission, we roughly take $\sigma_{\text{dl}} \sim \sigma_1$.) Other parameters include $\gamma_L = 150 \text{ MHz}$ and $r_A/\gamma = 3$, where γ_L is the laser linewidth [full width at half maximum (FWHM)] and r_A is the lamp's photon absorption rate out of $F_g = 2$. Consistent with experiment we see that the lamp RIN is larger for the laser tuned to $F_g = 1$ (i.e., $\Delta_{\text{Laser}} \sim 5 \text{ GHz}$) than for the laser tuned to $F_g = 2$ (i.e., $\Delta_{\text{Laser}} \sim -2.5 \text{ GHz}$). Note, however, that the relationship between the RIN_{lamp} levels for the laser tuned to these two absorption lines is a function of r_A as illustrated in Fig. 8. There, we see that for low lamp intensities, RIN_{lamp} for $F_g = 2$ can be larger than for $F_g = 1$. This is explained by lamplight optical pumping: at high levels of r_A/γ the lamp optically pumps and removes atoms from $|F_g = 2\rangle$. Thus, no matter the laser's fluctuations there are few atoms in $|F_g = 2\rangle$ to be affected by laser noise; conversely, there are many atoms in $|F_g = 1\rangle$ to be affected by laser noise. Note that the crossover occurs for $r_A/\gamma = 0.5$, which suggests a

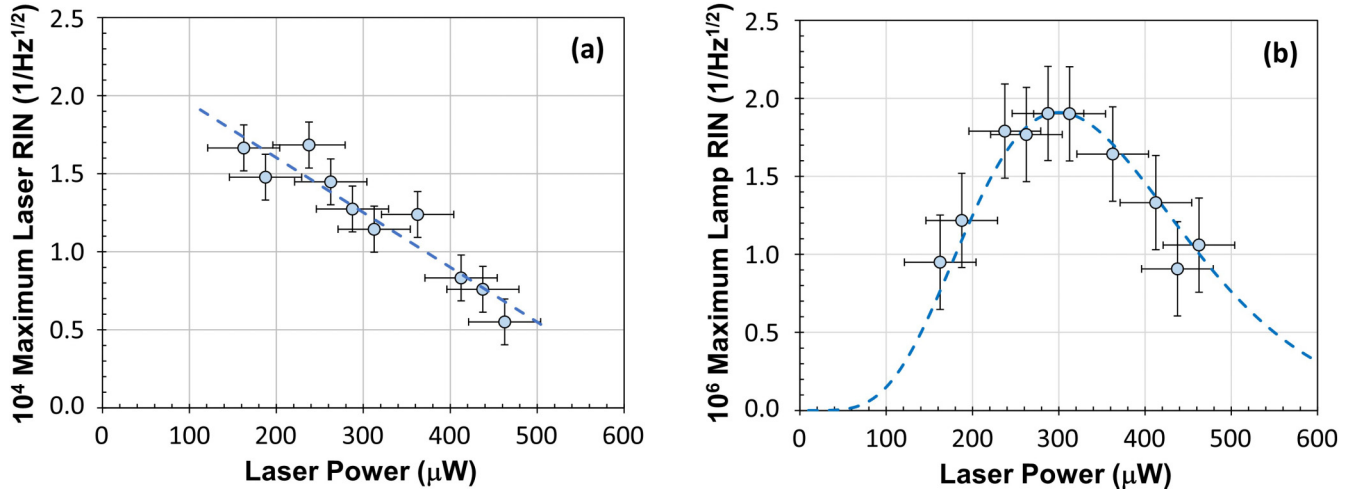


FIG. 5. (a) Maximum laser RIN/Hz^{1/2} as a function of laser power for the laser tuned to $|F_g = 1\rangle$, with the dashed line a least-squares straight-line fit simply meant as an aid to guide the eye. (b) Maximum lamp RIN/Hz^{1/2} as a function of laser power for the laser tuned to $|F_g = 1\rangle$, with the dashed line a least-squares fit to a Gamma distribution, again simply as an aid to guide the eye. (In the fit, we did not want to assume symmetry about the peak; thus, we choose a function that could accommodate asymmetry.) In both cases, a baseline RIN for the laser tuned off resonance has been subtracted from the data shown in Fig. 4.

lamp intensity of $\sim 30 \mu\text{W}$ (based on an equivalence with R_o/γ and the calibration discussed above). Since we expect alkali rf-discharge lamps to emit at least $\sim 50 \mu\text{W}$ (D_1 and D_2 combined) [36,37], Fig. 8 indicates that our rf-discharge lamp likely has sufficient photon flux for optical pumping (which has also been verified in separate experiments), and therefore that RIN_{lamp} (as observed) would be larger for the laser tuned to $F_g = 1$ than for the laser tuned to $F_g = 2$.

Figure 9 shows RIN_{lamp} as a function of laser power for $\gamma_L = 75$ MHz (dashed curve) and 150 MHz (solid curve), respectively. For both laser linewidths, which are in the range of expected VCSEL linewidths [25,26], RIN_{lamp} peaks at a

laser power of about $200 \mu\text{W}$, which is consistent with experiment [Fig. 5(b)]. Moreover, RIN_{lamp} for the laser tuned to $F_g = 2$ is about a factor of 3 smaller than for the laser tuned to $F_g = 1$, which is again consistent with experiment (see Fig. 4). Together Figs. 7–9 indicate that our experimental results are fully consistent with a RIN_{lamp} driven by PM-to-AM induced optical pumping noise. This suggests that at low noisy-field powers (where there is little optical pumping) and high noisy-field powers (where optical pumping saturates), there will be negligible PM-to-AM noise of any type on a quiet probe field.

V. SUMMARY

We have addressed the question of whether a phase-noisy field maps absorption cross-section fluctuations onto a quiet field, which has relevance to a host of (both basic and ap-

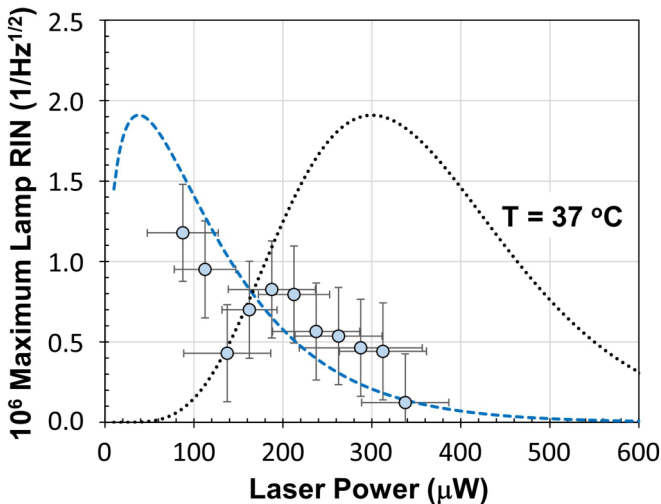


FIG. 6. Lamplight RIN for the laser tuned to $|F_g = 1\rangle$ as a function of laser power with $T = 30^\circ\text{C}$. The dashed line is a least-squares fit to a Gamma distribution, and again is only meant as an aid to guide the eye. However, similar to Fig. 5(b), and extrapolating from previous research [14], we assumed that the maximum value of the RIN for this fit would be independent of temperature. The fit from the 37°C data is shown for comparison.

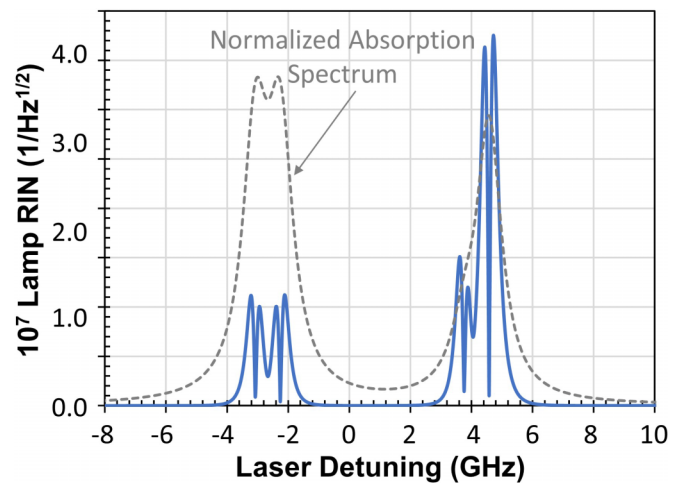


FIG. 7. Lamplight RIN for the laser tuned across the D_1 absorption line at 795 nm. For this computation, $T = 37^\circ\text{C}$, $P_{\text{laser}} = 200 \mu\text{W}$, $r_A/\gamma = 3$, and $\gamma_L = 150$ MHz.

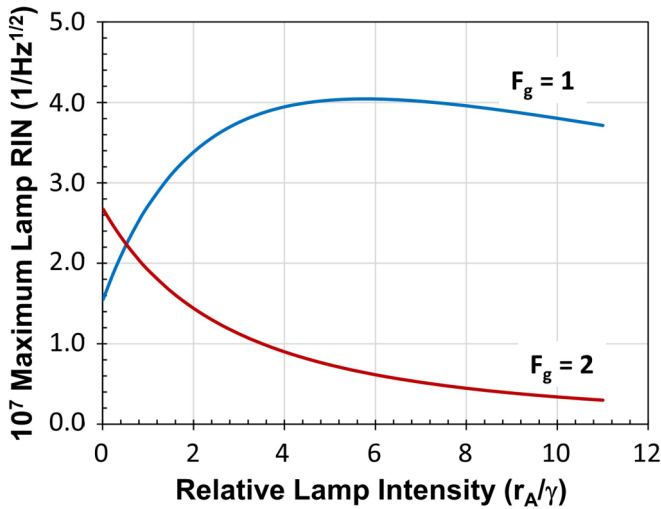


FIG. 8. Lamplight RIN for the laser tuned to either $F_g = 1$ or $F_g = 2$ as a function of the lamp's photon absorption rate, r_A/γ . For this computation, $T = 37^\circ\text{C}$, $P_{\text{laser}} = 200\ \mu\text{W}$, and $\gamma_L = 150\ \text{MHz}$.

plied) pump-probe atomic-molecular-optical (AMO) physics experiments. As particular examples of applied atomic technology applications, we note that PM-to-AM conversion is a dominant noise process (if not the dominant noise process) in a number of next-generation atomic clocks for global navigation satellite systems (GNSS): the lamp-laser integrated vapor-cell atomic clock [38], chip-scale atomic clocks [39], and the pulsed optically pumped atomic clock [40]. In the latter two cases, the present work suggests that there could be advantage in employing a phase-quiet field for the probe signal, since there can be no mapping of PM-to-AM noise from the pump onto the probe no matter the timescale of the probe-pump temporal separation.

In this regard, our results demonstrate that PM-to-AM noise does *not* transfer directly onto a quiet field, consistent with the notion that the atoms interacting with the noisy

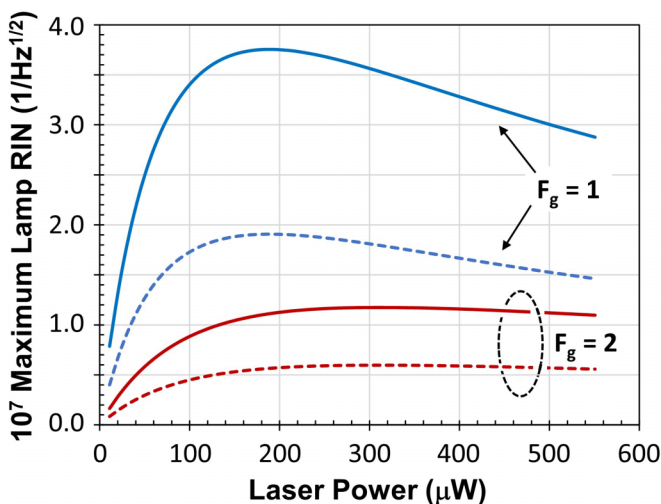


FIG. 9. Lamplight RIN for the laser tuned to either $F_g = 1$ or $F_g = 2$ as a function of laser power. For this computation $T = 37^\circ\text{C}$, $r_A/\gamma = 3$, and $\gamma_L = 150\ \text{MHz}$ (solid curve) or $75\ \text{MHz}$ (dashed curve).

field are instantaneously separate and distinct from those interacting with the quiet field. However, as a consequence of optical pumping, the noisy field can influence the quiet field's transmission through the vapor. As the noisy field undergoes PM-to-AM conversion, the noisy field's photon absorption rate fluctuates, which results in optical pumping rate fluctuations. With fluctuations in the rate of optical pumping come fluctuations in the number density of atoms in the states attenuating the quiet field's transmission. In a phrase, we have PM-to-AM *induced* optical pumping noise transfer to the quiet field. The saving grace for this type of noise transfer is that for very low noisy-field intensities (where there is no optical pumping) or very high noisy-field intensities (where optical pumping saturates) PM-to-AM induced optical pumping noise will be negligible. This is important for those next-generation GNSS atomic clocks noted above, since saturation of optical pumping, which will give the greatest atomic signals, coincides with the lowest levels of PM-to-AM induced optical pumping noise.

Finally, we note that in the present work we only considered PM-to-AM noise conversion at a relatively low Fourier frequency (i.e., 233 Hz). While this provides important information for next-generation GNSS clocks, which generate atomic signals at these low Fourier frequencies [38–40], it would be interesting from a basic atomic physics perspective to understand how PM-to-AM noise and PM-to-AM induced optical pumping noise map to an independent field as the Fourier frequency varies over a wide range, for example, 10^2 – $10^5\ \text{Hz}$. Since optical pumping timescales are typically on the order of $10^{-3}\ \text{s}$, one might imagine that at Fourier frequencies higher than $10^4\ \text{Hz}$ PM-to-AM induced optical pumping noise would no longer map to the independent field. Consequently, though the present results are important in themselves, we expect to conduct PM-to-AM noise and PM-to-AM induced optical pumping noise studies over a very broad Fourier frequency range in the not too distant future.

ACKNOWLEDGMENTS

The authors thank Daniele Monahan and Zachary Warren for stimulating discussions regarding PM-to-AM noise conversion. This work was funded by the U.S. Space Force Space Systems Command under Contract No. FA8802-19-C-0001.

APPENDIX: THEORY OF PM-TO-AM INDUCED OPTICAL PUMPING NOISE

Figure 10 shows the four-level model we consider in our analysis of PM-to-AM induced optical pumping noise. For simplicity, we assume that the lamplight only probes atoms in level $|2\rangle$ (i.e., $|F_g = 2\rangle$), while the laser tunes across the four optical absorption lines indicated in the figure. Our goal will be to compute the fractional population variation of $|2\rangle$, $\delta\rho_2$, which then becomes a measure of the lamplight noise on the photodetector:

$$S_{\text{Lamp}} = I_o e^{-(\rho_2 + \delta\rho_2)[\text{Rb}]\sigma_{\text{dl}}L} \Rightarrow \text{RIN}_{\text{Lamp}} \sim \delta\rho_2[\text{Rb}]\sigma_{\text{dl}}L. \quad (\text{A1})$$

Since lamp-pumped Rb atomic frequency standards are limited in the short term by shot noise [27], we will assume

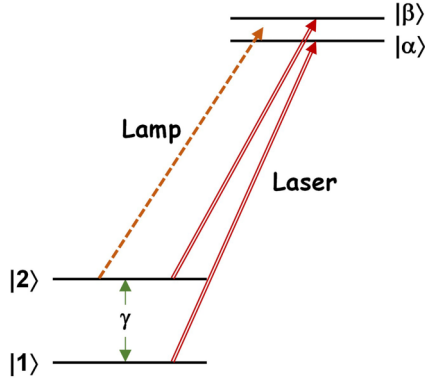


FIG. 10. Energy level diagram for our model. The lamp only excites atoms out of $|2\rangle$, so that the lamp's RIN is defined by population fluctuations in $|2\rangle$.

that the lamplight has no PM-to-AM conversion noise of its own, and that the only contribution to lamplight RIN comes from fluctuations in the population density of $|2\rangle$.

To proceed, we take the fractional populations in the two ground-state levels as $\rho_2^o = \frac{5}{8}$ for $|2\rangle$ and $\rho_1^o = \frac{3}{8}$ for $|1\rangle$ in the absence of lamp and laser light, and we define γ as the rate of collisional transfer between the two levels. We also assume that laser and lamp optical excitation is relatively slow compared to spontaneous emission from $|\alpha\rangle$ and $|\beta\rangle$, and that spontaneous emission branching ratios to $|2\rangle$ and $|1\rangle$ are equal. Thus, with ρ_j defined as the fractional population in $|j\rangle$ we have $\rho_1 + \rho_2 = 1$.

As the laser is tuned, there will be four distinct resonances for laser absorption. Ranging from lower to higher laser frequencies these are $|2\rangle \rightarrow |\alpha\rangle$, $|2\rangle \rightarrow |\beta\rangle$, $|1\rangle \rightarrow |\alpha\rangle$, and $|1\rangle \rightarrow |\beta\rangle$. These will be labeled as transitions 1–4, respectively, in what follows. We also note that the matrix elements for the transitions in ^{87}Rb imply that the relative excitation probabilities for transitions 1 and 2 are the same ($\eta_1 = \eta_2 = 1.0$), while the relative excitation probability for transition 3 has $\eta_3 = 0.33$ and $\eta_4 = 1.67$.

1. Optical pumping rate equation for ρ_2

The density-matrix equation for the evolution of ρ_2 in steady state can be written as

$$\frac{d\rho_2}{dt} = 0 = -\frac{1}{2} \sum_{j=1}^2 R_j \rho_2 + \frac{1}{2} \sum_{j=3}^4 R_j (1 - \rho_2) - \frac{r_A}{2} \rho_2 + \gamma (\rho_2^o - \rho_2). \quad (\text{A2})$$

Here, r_A is the excitation rate associated with the lamplight (which includes excitation to both excited-state hyperfine levels given the lamp's spectral linewidth), and the R_j are excitations associated with the laser,

$$R_j = \Phi \sigma_j = \frac{\Phi \sigma_o \eta_j \Gamma^2}{\Gamma^2 + \Delta_j^2} = R_o \eta_j g_j, \quad (\text{A3})$$

where $\eta_j \Phi \sigma_o = \eta_j R_o$ is the on-resonance photon absorption rate for the various transitions (given a laser photon flux Φ and with the D_1 absorption cross section given by σ_o), $g_j = \Gamma^2 / (\Gamma^2 + \Delta_j^2)$, and η_j is the relative strength of absorption for each of the transitions noted above. Equation (A2) yields

for the steady-state population in $|2\rangle$,

$$\rho_2 = \frac{R_3 + R_4 + 2\gamma \rho_2^o}{\sum_{j=1}^4 R_j + r_A + 2\gamma} \Rightarrow \frac{R_3 + R_4 + 2\rho_2^o}{\sum_{j=1}^4 R_j + r_A + 2}. \quad (\text{A4})$$

In the expression on the right-hand side of Eq. (A4), all rates have been normalized in terms of the collisional longitudinal relaxation rate: $R_o/\gamma \rightarrow R_o$ and $r_A/\gamma \rightarrow r_A$.

2. Including PM-to-AM conversion

PM-to-AM conversion will cause the absorption cross sections of the four transitions to fluctuate as the laser is tuned across resonance, giving rise to fluctuations in all of the R_j : $\sigma_j \rightarrow \bar{\sigma}_j + \delta\sigma_j$, where $\bar{\sigma}_j$ is the time-averaged absorption cross section for transition j (with the $\delta\sigma_j$ mean-zero random fluctuations). In turn, we have $R_j = \bar{R}_j + \delta R_j = \bar{R}_j + R_o \eta_j g_j (\delta\sigma_j/\sigma_o)$ or $R_j = \bar{R}_j + R_o \eta_j x_j g_j$. Here, x_j is a mean-zero random fluctuation in the *normalized* photon absorption cross section that varies (in addition to the g_j term) as the laser is tuned across one of the four resonances.

As suggested by the experiments reported here, we assume that these cross-section fluctuations only affect the absorption of laser light. They have no effect on the absorption cross section of lamplight photons. This assumption follows from several caveats:

(1) There is no long-range atom-atom interaction. Thus, light-induced perturbations that act on one atom are not transmitted to another atom due to long-range atom-atom couplings.

(2) Absorption cross-section fluctuations arise from the superposition state that is created in an individual atom when it absorbs an individual photon. Thus, PM-to-AM conversion is a process that happens to *single atoms*. It is only in the aggregate that these manifest as absorption cross-section fluctuations for the vapor as a whole.

(3) For the photon absorption rates that we consider there is negligible (effectively zero) probability for an atom to interact with a laser photon while it is interacting with a lamplight photon.

To account for the fluctuations in ρ_2 that arise from laser PM-to-AM noise conversion we expand ρ_2 in a Taylor series about $x_j = 0$. Effectively, we are performing a coarse-grained time average over the density-matrix rate equations [i.e., Eqs. (A2)], allowing the density matrix to reach steady state prior to any change in the randomly fluctuating cross section. This is likely fair if the lock-in amplifier reference frequency of Fig. 1, f_{Ref} , is chosen so that $f_{\text{Ref}} \sim \gamma$ or less. Thus, we write

$$\begin{aligned} \rho_2(\vec{x}) &= \bar{\rho}_2 + \sum_{j=1}^4 x_j \left. \frac{\partial \rho_2}{\partial x_j} \right|_{x_j=0} + \dots \\ &= \bar{\rho}_2 + \sum_{j=1}^4 x_j \left. \frac{dR_j}{dx_j} \frac{\partial \rho_2}{\partial R_j} \right|_{x_j=0} + \dots \end{aligned} \quad (\text{A5})$$

Considering an optically thin vapor, where we can take the x_j as small, we retain only first-order terms in Eq. (A5) so that

$$\rho_2(\vec{x}) \cong \bar{\rho}_2 + \sum_{j=1}^4 R_o \eta_j x_j g_j \frac{\partial \rho_2}{\partial R_j}. \quad (\text{A6})$$

From Eq. (A4) we then evaluate the $\partial\rho_2/\partial R_j$:

$$\frac{\partial\rho_2}{\partial R_j} = \begin{cases} \frac{-\langle\bar{R}_3+\bar{R}_4+2\rho_2^o\rangle}{\left[\sum_{k=1}^4\bar{R}_k+r_A+2\right]^2} & \text{for } j=1,2 \\ \frac{\bar{R}_1+\bar{R}_2+r_A+2(1-\rho_2^o)}{\left[\sum_{k=1}^4\bar{R}_k+r_A+2\right]^2} & \text{for } j=3,4 \end{cases}. \quad (\text{A7})$$

This can be simplified further by noting from Eq. (A4) that

$$\bar{\rho}_2 = \frac{\bar{R}_3 + \bar{R}_4 + 2\rho_2^o}{\sum_{k=1}^4 \bar{R}_k + r_A + 2}, \quad (\text{A8})$$

which results in

$$\frac{\partial\rho_2}{\partial R_j} = \begin{cases} \frac{-\bar{\rho}_2}{\left[\sum_{k=1}^4\bar{R}_k+r_A+2\right]} & \text{for } j=1,2 \\ \frac{1-\bar{\rho}_2}{\left[\sum_{k=1}^4\bar{R}_k+r_A+2\right]} & \text{for } j=3,4 \end{cases}. \quad (\text{A9})$$

Finally, employing Eq. (A9) in Eq. (A6) we obtain

$$\delta\rho_2 = \frac{R_o}{\Lambda} [(1-\bar{\rho}_2)(\eta_3x_3g_3 + \eta_4x_4g_4) - \bar{\rho}_2(\eta_1x_1g_1 + \eta_2x_2g_2)], \quad (\text{A10})$$

with

$$\Lambda \equiv \sum_{k=1}^4 \bar{R}_k + r_A + 2. \quad (\text{A11})$$

Note that with the x_j as mean zero we see from Eq. (A11) that we get the intuitively pleasing result $\langle\delta\rho_2\rangle = 0$, where $\langle\cdots\rangle$ indicates an ensemble average.

a. Variance of ρ_2 under laser PM to AM

As the mean value of $\delta\rho_2$ is zero, the variance of ρ_2 will be given by $\langle\rho_2^2\rangle$. Squaring Eq. (A10) and taking an ensemble average, we obtain

$$\begin{aligned} \langle\delta\rho_2^2\rangle = & \left(\frac{R_o}{\Lambda}\right)^2 \left\{ (1-\langle\rho_2\rangle)^2 (\eta_3^2\langle x_3^2\rangle g_3^2 + \eta_4^2\langle x_4^2\rangle g_4^2 \right. \\ & + 2\eta_3\eta_4\langle x_3x_4\rangle g_3g_4) + \langle\rho_2\rangle^2 (\eta_1^2\langle x_1^2\rangle g_1^2 + \eta_2^2\langle x_2^2\rangle g_2^2 \\ & \left. + 2\eta_1\eta_2\langle x_1x_2\rangle g_1g_2) \right\}. \quad (\text{A12}) \end{aligned}$$

Since the laser will tune to different resonances at different times, the laser PM fluctuations occurring (for example) when the laser is tuned to the $|1\rangle \rightarrow |\alpha\rangle$ transition will be

uncorrelated with the laser PM fluctuations when the laser is tuned to the $|2\rangle \rightarrow |\alpha\rangle$ transition. Thus, we set $\langle x_1x_3\rangle = \langle x_1x_4\rangle = \langle x_2x_3\rangle = \langle x_2x_4\rangle = 0$. However, because the transitions $|2\rangle \rightarrow |\alpha\rangle$ and $|\beta\rangle$ overlap as well as the transitions $|1\rangle \rightarrow |\alpha\rangle$ and $|\beta\rangle$, laser PM at any instant of time will affect both photon absorption rates simultaneously. Consequently, we have retained a correlation for the overlapped transitions: $\langle x_1x_2\rangle \neq 0$ and $\langle x_3x_4\rangle \neq 0$.

Note that this correlation will be strongest when the laser is tuned midway between the α and β states. This implies that a PM fluctuation that results in a positive detuning for one of the closely spaced transitions will result in a negative detuning for the other closely spaced transition. Therefore, we expect this correlation to be negative in a regime of laser tuning that produces non-negligible levels of correlation.

To evaluate Eq. (A12), $\langle x_j^2\rangle$ is taken from Huang *et al.* [41]:

$$\langle x_j^2\rangle = 6.4B\Delta_j^2 \frac{\Gamma^3\gamma_L(A+\gamma_L)}{(\Gamma^2+4\Delta_j^2)^4}. \quad (\text{A13})$$

Here, B is the measurement bandwidth set by the lock-in amplifier (typically 1 Hz), γ_L is the laser linewidth (FWHM), A is the Einstein-A coefficient for the transition, and Γ is the linewidth of the transition (FWHM). For the nonzero correlations in Eq. (A12) we make the approximation that

$$\langle x_ix_j\rangle g_ig_j \cong -g_ig_j\sqrt{\langle x_i^2\rangle\langle x_j^2\rangle}, \quad (\text{A14})$$

which is clearly only significant when the laser is tuned *between* the i th and j th transitions.

It is worth noting in Eq. (A12) that the variance in the population fluctuations of $|2\rangle$ (i.e., the lamp probed state) depends on two factors: the mean population in state $|2\rangle$ and the variance of absorption cross-section fluctuations. In particular, note that the amplitude of state $|2\rangle$ population fluctuations with the laser tuned to transitions 1 and 2 (i.e., $|2\rangle \rightarrow |\alpha\rangle$ and $|\beta\rangle$) depends on the population in $|2\rangle$, which is reduced by optical pumping. Similarly, the amplitude of population fluctuations with the laser tuned to transitions 3 and 4 (i.e., $|1\rangle \rightarrow |\alpha\rangle$ and $|\beta\rangle$) depends on the population in $|1\rangle$ (i.e., $1-\langle\rho_2\rangle$), which is again reduced by optical pumping. Consequently, at high laser optical pumping rates, so that $\langle\rho_2\rangle$ is zero (with the laser tuned to $|2\rangle \rightarrow |\alpha\rangle$ and $|\beta\rangle$) or unity (with the laser tuned to $|1\rangle \rightarrow |\alpha\rangle$ and $|\beta\rangle$), there will be no population fluctuations of $|2\rangle$ and hence no PM-to-AM induced variations in the transmitted lamplight.

- [1] A. Corney, *Atomic and Laser Spectroscopy* (Clarendon Press, Oxford, 1977); W. H. Louisell, *Quantum Statistical Properties of Radiation* (John Wiley & Sons, New York, 1973); J. I. Steinfeld, *Molecules and Radiation* (The MIT Press, Cambridge, MA, 1974).
- [2] P. Siddons, Light propagation through atomic vapours, *J. Phys. B: At., Mol. Opt. Phys.* **47**, 093001 (2014).
- [3] H. Jeong, A. M. C. Dawes, and D. J. Gauthier, Direct Observation of Optical Precursors in a Region of Anomalous Dispersion, *Phys. Rev. Lett.* **96**, 143901 (2006).

- [4] J. D. Jackson, *Classical Electrodynamics* (John Wiley & Sons, New York, 1975), Chap. 7.
- [5] M. Schwartz, *Principles of Electrodynamics* (McGraw-Hill, New York, 1972), Chap. 10.
- [6] P. R. Berman and R. Salomaa, Comparison between dressed-atom and bare-atom pictures in laser spectroscopy, *Phys. Rev. A* **25**, 2667 (1982).
- [7] J. Camparo, The semiclassical stochastic-field/atom interaction problem, in *Proceedings of the 7th Symposium on Frequency Standards and Metrology*, edited by L. Maleki (World Scientific, Hackensack, NJ, 2009) pp. 109–117.

- [8] Y. Sun and C. Zhang, Stochasticity in narrow transitions induced by laser noise, *Phys. Rev. A* **89**, 032516 (2014).
- [9] A. Papoyan and S. Shmavonyan, Signature of optical Rabi oscillations in transmission signal of atomic vapor under continuous-wave laser excitation, *Opt. Commun.* **482**, 126561 (2021).
- [10] Y. Xiao, T. Wang, M. Baryakhtar, M. Van Camp, M. Crescimanno, M. Hohensee, L. Jiang, D. F. Phillips, M. D. Lukin, S. F. Yelin, and R. L. Walsworth, Electromagnetically induced transparency with noise lasers, *Phys. Rev. A* **80**, 041805(R) (2009).
- [11] Y. Xiao, M. Baryakhtar, D. F. Phillips, and R. L. Walsworth, Conversion of phase noise to intensity noise in electromagnetically induced transparency, *Proc. SPIE* **7612**, 761209 (2010).
- [12] I. Yavuz, Z. Altun, and T. Topcu, Enhancement of high-order harmonic generation in the presence of noise, *J. Phys. B: At., Mol. Opt. Phys.* **44**, 135403 (2011).
- [13] G. M. Nikolopoulos and P. Lambropoulos, Effects of free-electron-laser field fluctuations on the frequency response of driven atomic resonances, *Phys. Rev. A* **86**, 033420 (2012).
- [14] J. C. Camparo, Conversion of laser phase noise to amplitude noise in an optically thick vapor, *J. Opt. Soc. Am. B* **15**, 1177 (1998).
- [15] S. Micalizio, C. E. Calosso, A. Godone, and F. Levi, Metrological characterization of the pulsed Rb clock with optical detection, *Metrologia* **49**, 425 (2012).
- [16] T. Bandi, C. Affolderbach, C. Stefanucci, F. Merli, A. K. Skrivervik, and G. Miletì, Compact high-performance continuous-wave double-resonance rubidium standard with $1.4 \times 10^{-13} \tau^{-1/2}$ stability, *IEEE Trans. Ultrason., Ferroelectr., Freq. Control* **61**, 1769 (2014).
- [17] J. G. Coffer, M. Anderson, and J. C. Camparo, Collisional dephasing and the reduction of laser phase-noise to amplitude-noise conversion in a resonant atomic vapor, *Phys. Rev. A* **65**, 033807 (2002).
- [18] Consider a vapor that has a length of several centimeters. The time for a wavefront to pass through this medium will be ~ 100 ps. For a laser with a linewidth of 50 MHz (typical for a VCSEL diode laser), the correlation time of the field will be ~ 6 ns.
- [19] J. C. Camparo and J. G. Coffer, Conversion of laser phase noise to amplitude noise in a resonant atomic vapor: The role of laser linewidth, *Phys. Rev. A* **59**, 728 (1999).
- [20] P. Burdekin, S. Grandi, R. Newbold, R. A. Hogarth, K. D. Major, and A. S. Clark, Single-Photon-Level Sub-Doppler Pump-Probe Spectroscopy of Rubidium, *Phys. Rev. Appl.* **14**, 044046 (2020).
- [21] L. Guillemot, P. Loiko, J.-L. Doualan, A. Braud, and P. Camy, Excited-state absorption in thulium-doped materials in the near-infrared, *Opt. Express* **30**, 31669 (2022).
- [22] J. C. de Aquino Carvalho, I. Maurin, H. Failache, D. Bloch, and A. Laliotis, Velocity preserving transfer between highly excited atomic states: Black body radiation and collisions, *J. Phys. B: At., Mol. Opt. Phys.* **54**, 035203 (2021).
- [23] W. E. Bell, A. L. Bloom, and J. Lynch, Alkali metal vapor spectral lamps, *Rev. Sci. Instrum.* **32**, 688 (1961).
- [24] V. B. Gerard, Laboratory alkali metal vapour lamps for optical pumping experiments, *J. Sci. Instrum.* **39**, 217 (1962).
- [25] D. Kuksenkov, S. Feld, C. Wilmsen, and H. Temkin, Linewidth and α -factor in AlGaAs/GaAs vertical cavity surface emitting lasers, *Appl. Phys. Lett.* **66**, 277 (1995).
- [26] S. Viciani, M. Gabrysch, F. Marin, F. Monti di Sopra, M. Moser, and K. H. Gulden, Lineshape of a vertical cavity surface emitting laser, *Opt. Commun.* **206**, 89 (2002).
- [27] J. Vanier and L.-G. Bernier, On the signal-to-noise ratio and short-term stability of passive rubidium frequency standards, *IEEE Trans. Instrum. Meas.* **30**, 277 (1981).
- [28] In vapor-cell clocks, one generally wants to operate at the onset of saturation, where the Rabi frequency, Ω , is approximately equal to the dephasing rate, $1/T_2$. This produces the largest signal, while at the same time generating a large atomic Q ; in alkali vapor-cell atomic clocks one generally finds $1/T_2 \sim 10^2$ Hz. As discussed in the following Ref. [29], the largest modulated response of an atom to a phase modulated field occurs when the modulation frequency is nearly equal to Ω .
- [29] J. C. Camparo and R. P. Frueholz, Observation of the Rabi-resonance spectrum, *Phys. Rev. A* **38**, 6143 (1988).
- [30] N. Kuramochi, I. Matsuda, and H. Fukuyo, Analysis of the effect of foreign gases in the filtering action of a ^{85}Rb cell, *J. Opt. Soc. Am.* **68**, 1087 (1978).
- [31] J. Vanier, R. Kunski, P. Paulin, M. Têtu, and N. Cyr, On the light shift in optical pumping of rubidium 87: The techniques of “separated” and “integrated” hyperfine filtering, *Can. J. Phys.* **60**, 1396 (1982).
- [32] P. Atkins, *Physical Chemistry* (W.H. Freeman and Co., New York, 1998), Chap. 16.
- [33] We must recognize that due to the difference in linewidth for the lamplight and the laser light, the absorption cross sections will also be different.
- [34] J. Kitching, H. G. Robinson, L. Hollberg, S. Knappe, and R. Wynands, Optical-pumping noise in laser-pumped, all-optical microwave frequency references, *J. Opt. Soc. Am. B* **18**, 1676 (2001).
- [35] A. Hudson and J. Camparo, Mesoscopic physics in vapor-phase atomic systems: Collision shift gradients and the 0-0 hyperfine transition, *Phys. Rev. A* **98**, 042510 (2018).
- [36] J. C. Camparo and R. P. Frueholz, A nonempirical model of the gas-cell atomic frequency standard, *J. Appl. Phys.* **59**, 301 (1986).
- [37] T. N. Bandi and the Clock Team, Advanced space rubidium atomic frequency standard for satellite navigation, *GPS Solutions* **26**, 54 (2022).
- [38] M. Huang, A. Little, and J. Camparo, LaLI-POP: Lamp and laser integrated pulsed-optically pumped atomic clock, in *Proceedings of the 2022 Joint Conference of the European Frequency and Time Forum and IEEE International Frequency Control Symposium* (IEEE Press, Piscataway, NJ, 2022).
- [39] M. A. Hafiz, G. Coget, M. Petersen, C. E. Calosso, S. Guérandel, E. de Clercq, and R. Boudot, Symmetric autobalanced Ramsey interrogation for high-performance coherent-population-trapping vapor-cell atomic clock, *Appl. Phys. Lett.* **112**, 244102 (2018).
- [40] S. Macalizio, F. Levi, C. E. Calosso, M. Gozzelino, and A. Godone, A pulsed-laser Rb atomic frequency standard for GNSS applications, *GPS Solutions* **25**, 94 (2021).
- [41] M. Huang, J. G. Coffer, and J. C. Camparo, Absorption cross-section fluctuations driven by continuous and discrete laser frequency variations, *Opt. Commun.* **265**, 187 (2006).